

# Membrane potential generation without ion transport

Hirohisa Tamagawa

Received: 13 March 2014 / Revised: 25 November 2014 / Accepted: 26 November 2014 / Published online: 30 December 2014  
© Springer-Verlag Berlin Heidelberg 2014

**Abstract** Current view about cell is that the cell is a watery solution coated with semi-permeable membrane and there exists nonzero potential, so-called membrane potential, across the semi-permeable cell membrane. Goldman-Hodgkin-Katz equation and Donnan theory are the fundamental existing theories for explaining the cause of membrane potential generation. However, the observations of membrane potential inexplicable by these existing theories have been repeatedly reported by a small number of researchers for more than the past half century. Hence, it is needless to say important to reconsider the membrane potential generation mechanism. Based on the experimental result shown in this paper, it was concluded that the existing theories were not genuinely right for the explanation of membrane potential generation. Adsorption theory is only a genuinely right theory instead. The adsorption theory describes that the adsorption of the mobile ions on the adsorption sites on the membrane generates the membrane potential. This work introduces the experimental observation inexplicable by Goldman-Hodgkin-Katz equation or Donnan theory but is in harmony with the adsorption theory.

**Keywords** Membrane potential · Goldman-Hodgkin-Katz equation · Donnan theory · Ion adsorption

## Introduction

Membrane potential is the potential generated across a cell membrane [1–3]. It changes in accordance with the cell activity. Thus, the membrane potential is one of the indications of

the cell's biological activities. Goldman-Hodgkin-Katz equation (GHK equation) [1–3] and Donnan theory [1, 2, 4–6] are well-known concepts of membrane potential generation mechanisms. GHK equation describes the permeation rate of mobile ions through the cell membrane, and individual ion concentrations are fundamental factors in determining the membrane potential. Donnan theory describes that the membrane potential is generated by asymmetric ion distribution between cell inside and outside due to the existence of immobile ions to which the cell membrane is impermeable [1, 2, 4–6]. Both theories—GHK equation and Donnan theory—have been successfully employed in predicting the membrane potential behaviors in the recent past [1–6]. Virtually, no one has doubted these existing theories of membrane potential generation mechanism. However, a small number of researchers outside mainstream have continuously objected to these theories [1, 2, 6–8]. The leading scientist among those researchers is a physiologist, Dr. Gilbert Ling. He has explained the drawbacks of existing theories and advocated his own theory of membrane potential generation mechanism. According to his theory, the membrane potential is generated by the immobilization of mobile ions [1, 2, 6]. Mobile ions are immobilized because of their adsorption on the surfaces of substances constituting the cell, resulting in the nonzero membrane potential.

Independently of Dr. Ling, Dr. Kan Lu Cheng, an electrochemist, proposed a quite similar theory of potential generation mechanism of ion selective electrode such as a glass electrode [9–13]. Dr. Cheng's theory describes that the potential detected by the electrode is caused by the adsorption of ions on the electrode surface. He emphasized that the adsorbed ions (immobilized ions) forms a capacitor on the electrode surface, resulting in the potential generation.

In this paper, the author raises a question again against the existing theory of membrane potential generation mechanism and introduces some experimental evidences

H. Tamagawa (✉)  
Department of Mechanical Engineering, Faculty of Engineering,  
Gifu University, 1-1 Yanagido, Gifu, Gifu 501-1193, Japan  
e-mail: tmgwhrhs@gifu-u.ac.jp

in harmony with the theories advocated by Drs. Ling and Cheng [1, 2, 6, 9–13].

### Theories for membrane potential generation

In this section, the existing theories of the membrane potential generation mechanism and an alternative theory advocated by Drs. Ling and Cheng are introduced. The existing theories to be described are GHK equation [1–3] and the Donnan theory [1, 2, 4–6], and the alternative theory is called the adsorption theory [1, 2, 6, 9–13].

#### Existing theory

##### Goldman-Hodgkin-Katz equation

Considering that two aqueous solutions are separated by a semi-permeable membrane as illustrated in Fig. 1, both left and right compartments contain the ions  $X^+$  and  $Y^-$ . Potential of  $V$ , which is the potential in the left compartment in reference to the right compartment, across the semi-permeable membrane, is represented by the GHK equation of Eq. (1).

$$V = -\frac{RT}{F} \ln \left[ \frac{P_X[X^+]_l + P_Y[Y^-]_l}{P_X[X^+]_r + P_Y[Y^-]_r} \right] \quad (1)$$

$V$ : potential,  $R$ : gas constant,  $T$ : absolute temperature,  $F$ : Faraday constant,  $[m]_n$ : Concentration of  $m$  in  $n$ -compartment, when  $m$  is  $X^+$  or  $Y^-$ , and  $n$  is  $l$  (left) or  $r$  (right),  $P_m$ : Permeability constant of  $m$ , which represents the degree of semi-permeable membrane permeability to  $m$ .

The GHK equation implies that the potential generated across the semi-permeable membrane is dominated by the degree of ion transport through the semi-permeable membrane and the ion concentration [1–3]. Without ion transport through the membrane, the GHK equation is invalid for any system.

It is widely accepted that the ion transport through the cell membrane is caused not only by passive transport but also by

active transport [1–3]. The current and widely accepted concept of cell biology implies that ions are transported through the cell membrane by way of ion channels and pumps embedded in the cell membrane [1–3, 6, 7]. The passive ion transport through the cell membrane is caused by the diffusion of ions passing through the ion channels. The pump transports the ions through the cell membrane against the gradient of ion concentration, that is, the active transport [1, 2, 6, 7]. Regardless of whether passive or active transport, GHK equation precisely predicts the membrane potential behavior as long as the ion transport through the cell membrane is induced.

#### Donnan theory

Considering that the two aqueous solutions are separated by semi-permeable membrane as illustrated in Fig. 2a. Initially, the left compartment contains ions  $A^+$  and  $B^-$ , while the right compartment contains  $\alpha^+$  and  $\beta^-$ . The semi-permeable membrane is impermeable to  $A^+$  but permeable to the rest of ions. Because of the entrapment of  $A^+$  within the left compartment, the disparity of ion concentration between the left and right compartments is caused over time by the passive transport of ions of  $B^-$ ,  $\alpha^+$ , and  $\beta^-$  through the semi-permeable membrane. Such ion concentration disparity causes the electrical potential gradient—membrane potential—between the left and right compartments. Individual ion concentrations and electrical potential gradient come to settle at constant level, and such a state is the equilibrium state and illustrated in Fig. 2b. According to the Donnan theory, membrane potential across the semi-permeable membrane is the consequence of the asymmetric ion distribution between the left and right compartments caused by the existence of  $A^+$  impermeable to the semi-permeable membrane [1, 2, 4–6].

Basically, the abovementioned two existing theories require ion transport through the semi-permeable membrane more or less. The GHK equation given by Eq. (1) clearly contains  $P_m$  indicating the existence of ion transport. Even though the ion concentration in the left compartment is same as that in the right compartment, ion transport can take place as the equilibrium state ion transport. Hence, GHK equation is

**Fig. 1** Two ionic solutions separated with a semi-permeable membrane. Both left and right compartments contain the ions  $X^+$  and  $Y^-$ , but the concentration of  $X^+$  ( $Y^-$ ) in the left compartment is not necessarily the same as the concentration of  $X^+$  ( $Y^-$ ) in the right compartment

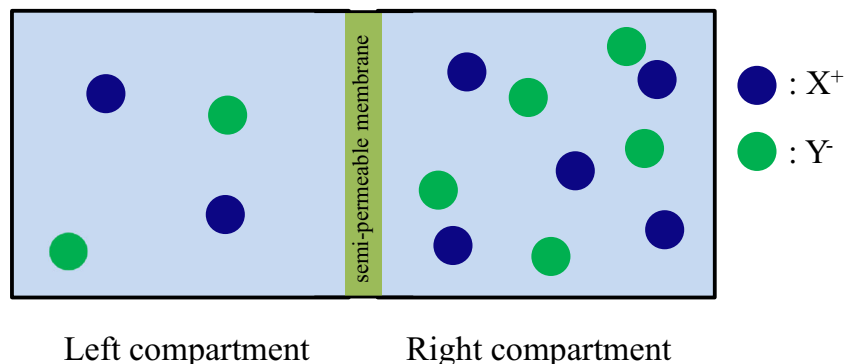
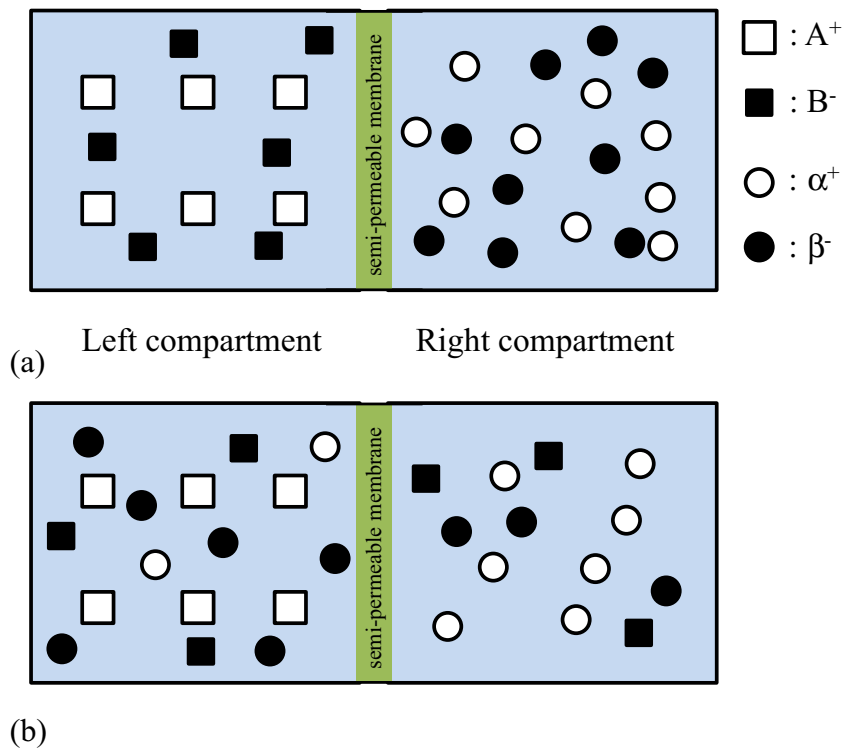


**Fig. 2** Two ionic solutions separated by a semi-permeable membrane. **a** Initially, the left compartment is filled with a solution containing substance AB which can dissociate into  $A^+$  and  $B^-$ , while the right compartment is filled with substance  $\alpha\beta$  which can dissociate into  $\alpha^+$  and  $\beta^-$ . The semi-permeable membrane is impermeable to  $A^+$  but permeable to the rest of the ions. **b** After a while, asymmetric ion distribution is realized because of entrapment of  $A^+$  within the left compartment



valid. However, without ion transport,  $P_m=0$ , GHK equation collapses. Donnan theory does not require continuous ion transport through the membrane. According to the Donnan theory, the nonzero potential across the membrane is caused merely by the asymmetric ion distribution as illustrated in Fig. 2b. As long as such an asymmetric ion distribution is achieved, the Donnan theory is valid, even though  $P_m=0$ . However, ion transport through the membrane should be induced at least once to realize the asymmetric ion distribution state (Fig. 2b) from the initial state of symmetric ion distribution (Fig. 2a). Therefore, the above two existing theories require more or less the ion transport through the membrane.

The adsorption theory

Basic concept of the adsorption theory is shown in this section. For the purpose of showing its essential part and achieving easy understanding, Dr. Cheng’s explanation is employed [9–13]. Imagine a glass membrane surface in contact with an aqueous solution containing protons, where the glass is the same type used for a glass electrode. Figure 3 illustrates the interfacial region between the glass surface and the aqueous solution containing protons. Protons are adsorbed onto the negatively charged sites of silanol groups on the glass membrane surface and form a positively charged layer as represented by the thin solid line in Fig. 3. Namely, silanol groups serve as adsorption sites for protons. The negatively charged adsorption sites of silanol groups form a negatively charged layer

represented by a dashed line in Fig. 3. The positively and negatively charged layers form a capacitor and potential  $\Phi$  is generated (see Fig. 3). This potential is detected by a glass electrode. So, the immobilization of protons due to their adsorption on the membrane surface is the origin of (membrane) potential. Furthermore, the glass membrane does not need to be permeable to ions for the membrane potential generation, the glass membrane only needs to bear adsorption sites on its surface. This alternative theory is hereafter called the adsorption theory.

According to the adsorption theory, even though two aqueous solutions are separated by an impermeable membrane such as the glass membrane, nonzero potential is generated

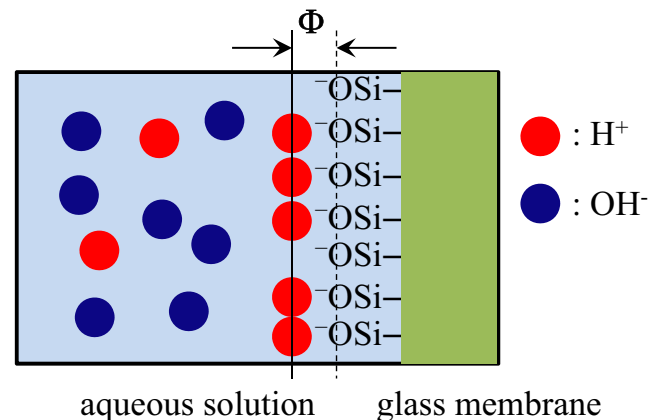


**Fig. 3** Interfacial structure between the glass membrane and an aqueous solution containing protons

across the glass membrane. Considering the two aqueous solutions containing protons separated by an impermeable glass membrane as illustrated in Fig. 4. Assuming that the proton concentration in the right solution is less than that in the left solution (see again Fig. 4), the capacitor formed on the right surface of the glass membrane is totally different from that formed on the left surface. Hence, the magnitude of potential generated on the right surface,  $\Phi'$ , is different from that on the left surface,  $\Phi$ . Hence, the consequently generated potential across the glass membrane is the nonzero potential of  $\Phi - \Phi' (\neq 0 \text{ V})$ . So, the adsorption theory does not require the ion transport at all for the nonzero potential induction.

Author of this paper, Tamagawa, and his collaborator, Morita, investigated the potential behavior across the impermeable membrane which separated two KCl solutions [14]. The potential behavior they observed was analyzed by their own theory. They prepared high and low concentration KCl solutions separated by a silver wire both ends of which were covered with AgCl serving as the adsorption sites for  $\text{Cl}^-$  as illustrated in Fig. 5. Because of the adsorption of  $\text{Cl}^-$  on the left surface of silver, the left surface of silver became negatively charged. Due to the negative charge, the ions of  $\text{K}^+$  and  $\text{Cl}^-$  in the left KCl solution came to inhomogeneously distribute by obeying the Boltzmann distribution. Hence, the potential represented by the dotted line drawn in the left KCl solution in Fig. 5 must have been generated. The same must be true for the right KCl solution, but the disparity of KCl concentration between the left and right KCl solutions caused the adsorption of larger quantity of  $\text{Cl}^-$  on the right surface of silver than on the left surface. It could consequently result in the potential in the right KCl solution, which was different from that in the left KCl solution as illustrated in Fig. 5. Potential in the left KCl solution at the immediate neighbor of silver abruptly changes in “ $\text{Cl}^-$  adsorption phase” (see Fig. 5). The potential reaches the bulk phase potential,  $\Phi_L$ , only a bit away from the left surface of silver. The same is true for the right KCl solution. When measuring the potential across a membrane, usually two electrodes are placed in the bulk phase of two solutions. One electrode is inserted into the bulk phase in the left solution, and another electrode is

inserted into the bulk phase in the right solution. Therefore, the potential in the system represented by Fig. 5 must be given by  $\Phi_L - \Phi_R$  according to Tamagawa and Morita's theory [14]. They successfully reproduced the experimentally observed potential behavior by the use of their theory. They concluded that the membrane potential was generated not by the permeation of ions through the membrane but by the inhomogeneous ion distribution, which obeyed the Boltzmann distribution, caused by the ion adsorption.

Dr. Ling's idea of cell membrane potential generation mechanism is basically the same as Dr. Cheng's [1, 2, 9–13], and Tamagawa and Morita's theory largely draws on the theories advocated by Drs. Ling and Cheng. Thus, Tamagawa and Morita concluded that the adsorption theory Drs. Ling and Cheng had advocated was a valid theory as the membrane potential generation mechanism.

A number of researchers might say that if the existing cell membrane potential generation mechanism is wrong, the foundation of contemporary concept of cell biology collapses. Therefore, it is quite natural for them to think that the adsorption theory is quite unlikely to be right. However, Dr. Ling's research results already provided the answers to such an issue and defied such doubts cast on the adsorption theory [1, 2, 5–7]. To introduce those Dr. Ling's answers is not the topic this paper deals with. This paper shows some experimental results contradicting the existing theory of membrane potential generation mechanism but in harmony with the adsorption theory advocated by Drs. Ling and Cheng.

## Experimental

In this paper, the author especially doubts the necessity of ion transport for the membrane potential generation. As described in the “Existing theory”, GHK equation is an explanation of membrane potential generation. It states that the potential generation is caused by the ion transport through the semi-permeable membrane. Donnan theory is another explanation of membrane potential generation mechanism, and it says that

**Fig. 4** Two aqueous solutions containing protons separated by an impermeable glass membrane. Proton concentration in the right solution is less than that in the left solution.  $\Phi'$  and  $\Phi$  ( $\Phi' \neq \Phi$ ) represent the potential generated on the right surface and left surface of the glass membrane, respectively

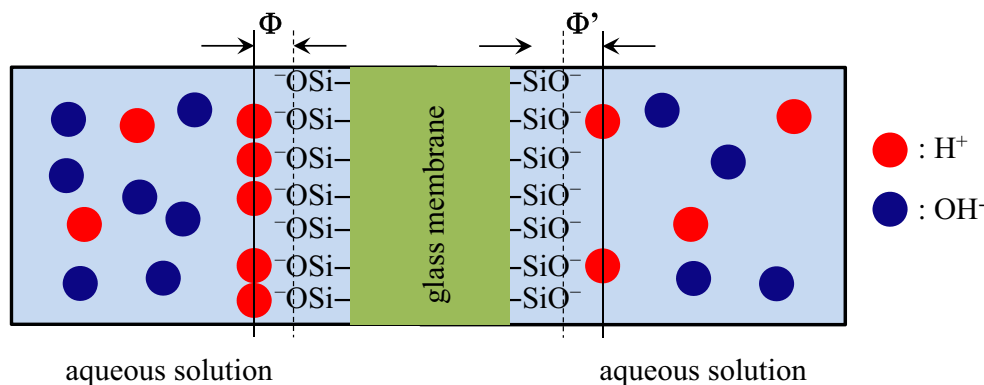
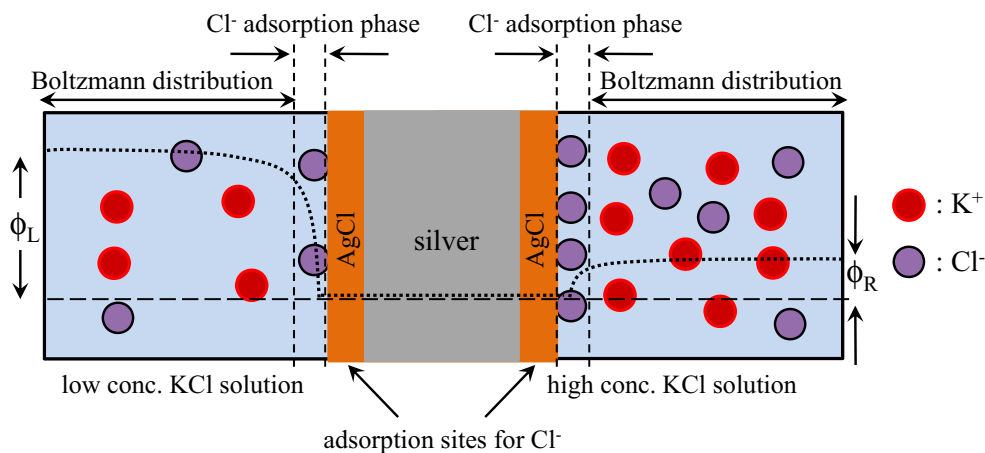


**Fig. 5** Two KCl solutions separated by a silver at both ends of which were covered with AgCl serving as the adsorption sites for Cl<sup>-</sup>. Dotted line represents the potential profile expected



the membrane potential is generated by the occurrence of asymmetric ion distribution as the consequence of ion transport through the semi-permeable membrane. Without the ion transport, neither GHK equation nor Donnan theory is applicable for explaining the membrane potential generation. Hence, in this study, the author especially focuses on the role of ion transport through the semi-permeable membrane for the membrane potential generation.

**Experimental setup**

The author scrutinized the membrane potential generation mechanism theoretically as well as experimentally. An experimental setup constituted of five compartments divided by four membranes, as illustrated in Fig. 6, was fabricated. The five compartments are denoted by N-compartment (North compartment), S-compartment (South compartment), W-compartment (West compartment), E-compartment (East compartment), and C-compartment (Center compartment), respectively. N-compartment and C-compartment are separated by the membrane denoted by N-C as in Fig. 6. Similarly, S-compartment and C-compartment, W-compartment and C-compartment, and E-compartment and C-compartment are separated by the membrane, S-C, W-C, and E-C, respectively. Figure 6 illustrates the setup for the measurement of potentials between N- and S-compartments by the voltmeter A and between W- and E-compartments by the voltmeter B.

**Preparation of solutions and membranes**

*Solution in N-, S-, W-, E-, and C-compartments*

In the experiments carried out, N-, S-, W-, and E-compartment were filled with KCl aqueous solutions. KCl solutions were prepared by dissolving KCl into deionized water. The condition for C-compartment is to be described in the “Results and discussion”.

*Membrane of N-C, S-C, W-C, and E-C*

*Semi-permeable membrane* The ion exchange membrane Selemion CMV was used for N-C, S-C, W-C, and E-C. It is manufactured by Asahi Glass Co. Ltd. (Tokyo) and commercially available. Selemion CMV contains fixed atomic group of -SO<sub>3</sub>H. Since -SO<sub>3</sub>H creates immobile anions of -SO<sub>3</sub><sup>-</sup> in the hydrated state, Selemion CMV works as a cation exchange membrane. It is used for the water purification, and the cations in the water are adsorbed on the Selemion CMV surface. Since Selemion CMV is a cation exchange membrane, it is quite obvious that anions hardly pass through Selemion CMV because of repulsive electrostatic force between the -SO<sub>3</sub><sup>-</sup> and the anions, while cations are adsorbed on Selemion CMV or easily pass through it because of attractive electrostatic

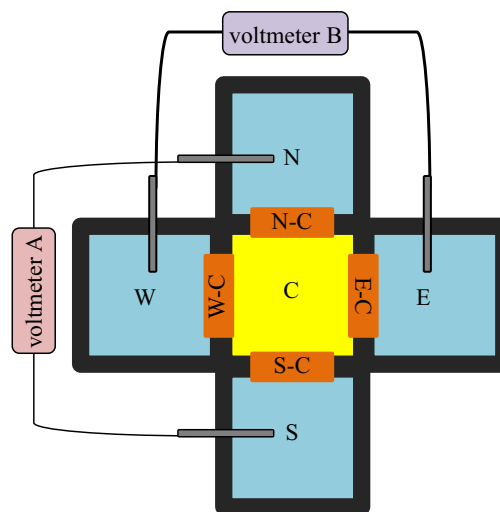


**Fig. 6** Experimental setup. The setup constitutes five compartments separated by four membranes. N, S, W, E, and C represent North-, South-, West-, East-, and Center-compartment, respectively. N-C, S-C, W-C, and E-C represent the membranes, respectively, separating neighboring two compartments. In this illustration, voltmeter A registers the potential between the N- and S-compartments, while voltmeter B registers the potential between the W and E-compartments

force between the  $-\text{SO}_3^-$  and the cations. Namely, Selemion CMV is a semi-permeable membrane. Thus, Selemion CMV was employed in this work as a model of semi-permeable membrane.

**Impermeable membrane** According to the adsorption theory, even though the membrane is impermeable to ions, the potential across the impermeable membrane is generated as long as the membrane surface has adsorption sites (see Fig. 4) [1, 2, 7, 9–14]. Therefore, it is important to experimentally study the behavior of potential across an impermeable membrane, too. In order to verify this concept of adsorption theory, the membranes to which  $\text{K}^+$  and  $\text{Cl}^-$  solution were impermeable and bearing surface adsorption sites for those ions were prepared. Using such membranes, the potential across the impermeable membrane was investigated. Similar experiment was already carried out by Colacicco about 50 years ago [1, 2, 14–16]. In the Colacicco's experiment, two ionic solutions were separated by an oil membrane. His membrane contained a minute quantity of detergent. Figure 7 illustrates the interface between the aqueous solution and oil membrane. Hydrocarbon tail of the detergent was anchored in the oil phase because of its hydrophobicity, while the charged head of the detergent protruded into aqueous solution because of its high affinity to water. Hence, the detergent molecules formed a monolayer as illustrated in Fig. 7. The charged head served as adsorption site for the ions bearing the charge of opposite sign to the head charge of the detergent. The oil membrane served as an impermeable membrane to ions. So, this membrane was an impermeable membrane bearing ion adsorption sites. With the Colacicco's experiments in mind, the author attempted to prepare oil membranes impermeable but bearing surface adsorption sites.

Two kinds of impermeable liquid membranes were prepared for this study. One was prepared by dissolving poly(ethylene glycol) 4-nonylphenyl 3-sulfopropyl ether potassium salt (hereafter called PEG-K) into 1-pentanol, where this liquid membrane is denoted Im-N. Once PEG-K dissociates, one end of PEG-K comes to have negative charge. Another one was prepared by dissolving 1-decyl-3-methylimidazolium

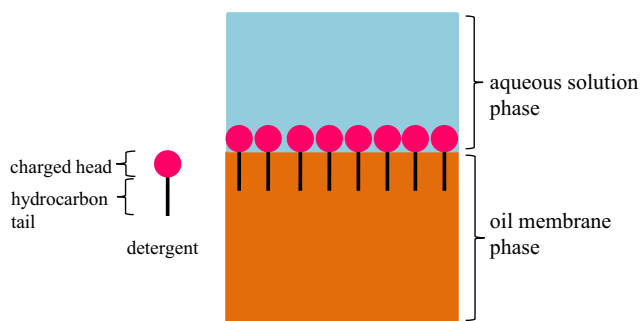


**Fig. 7** Detergent molecules forming a charged monolayer at the interface between aqueous solution and oil membrane

chloride (hereafter called DMIC) into 1-pentanol, where this liquid membrane is denoted Im-P. Once DMIC dissociates, one end of DMIC comes to have positive charge.

PEG-K and DMIC were chosen because of their long hydrocarbon tails and the charge at their heads. Owing to such long hydrocarbon tails, it was strongly expected that the monolayer of them were easily formed at the interface between the aqueous solution and the liquid membrane. It was expected that PEG-K would form a monolayer bearing negatively charged adsorption sites, while DMIC would form a monolayer bearing positively charged adsorption sites. So, the PEG-K monolayer would adsorb cations, while the DMIC monolayer would adsorb anions.

#### Experimental procedure—potential measurement

Typical experimental procedure is explained as follows: All the compartments shown in Fig. 6 were filled with KCl solutions. Neighboring KCl solutions were separated by the membranes N-C, S-W, W-C, and E-C. Which membrane, Selemion CMV or Im-N or Im-P, is used as N-C, S-W, W-C, and E-C depends on the experimental purpose. Potential was measured at room temperature in any experiment shown in this paper.

## Results and discussion

### Membrane potential across the semi-permeable membrane

#### Membrane potential in equilibrium state

Four pieces of Selemion CMV sheet were placed in the experimental setup (Fig. 6) as N-C, S-C, W-C, and E-C, respectively. All the compartments were filled up with KCl aqueous solutions, and their initial concentrations are shown in the row of “before” in Experiment 1 in Table 1. Then, the potentials,  $P_{N-S}$ ,  $P_{C-S}$ ,  $P_{W-E}$ , and  $P_{C-E}$ , in the equilibrium state were measured, where  $P_{i-j}$  represents the potential of  $i$ -compartment in reference to  $j$ -compartment. Right after filling all the compartments with KCl solutions, the potentials were unstable. But after a while, say after 10 s, the potentials settle at certain level, and this state is referred to as equilibrium state in this measurement. The potentials,  $P_{N-S}$ ,  $P_{C-S}$ ,  $P_{W-E}$ , and  $P_{C-E}$  are summarized in the row of “before” of Experiment 1 in Table 1. Then, the concentration of KCl solution in the W-compartment was disturbed on purpose by replacing the initial KCl solution in the W-compartment with a new KCl solution, and the potentials in the equilibrium state were measured again after the disturbance, where the concentration after the KCl solution replacement is shown in the row of “after” of Experiment 1 in Table 1. It was impossible to replace the

**Table 1** Concentration of KCl solution and potential generated before and after disturbance

Experiment 1 <sup>a</sup>						Potential <sup>c</sup> (mV)			
Concentration of KCl (M)						P <sub>N-S</sub>	P <sub>C-S</sub>	P <sub>W-E</sub>	P <sub>C-E</sub>
Compartment	N	S	W	E	C				
Before <sup>b</sup>	0.001	Sat. <sup>d</sup>	0.001	Sat.	1	140	27	139	28
After <sup>c</sup>	0.001	Sat.	Sat.	Sat.	1	139	27	4	27
Experiment 2 <sup>f</sup>						Potential <sup>c</sup> (mV)			
Concentration of KCl (M)						P <sub>N-S</sub>	P <sub>C-S</sub>	P <sub>W-E</sub>	P <sub>C-E</sub>
Compartment	N	S	W	E	C				
Before	0.001	Sat.	0.01	Sat.	1	129	27	121	27
After	0.001	Sat.	Sat.	Sat.	1	127	27	30	27
Experiment 3 <sup>g</sup>						Potential <sup>h</sup> (mV)			
Concentration of KCl (M)						P <sub>N-S</sub>	P <sub>C-S</sub>	P <sub>W-E</sub>	P <sub>C-E</sub>
Compartment	N	S	W	E	C				
Before	0.001	Sat.	0.01	Sat.	1	–	–	–	–
After	0.001	Sat.	Sat.	Sat.	1	–	–	–	–
Experiment 4 <sup>i</sup>						Potential <sup>j</sup> (mV)			
Concentration of KCl (M)						P <sub>N-S</sub>	P <sub>C-S</sub>	P <sub>W-E</sub>	P <sub>C-E</sub>
Compartment	N	S	W	E	C				
Before	0.001	Sat.	0.01	Sat.	0.00001	–	–	–	–
After	0.001	Sat.	Sat.	Sat.	0.00001	–	–	–	–
Experiment 5 <sup>k</sup>						Potential <sup>l</sup> (mV)			
Concentration of KCl (M)						P <sub>N-S</sub>	P <sub>C-S</sub>	P <sub>W-E</sub>	P <sub>C-E</sub>
Compartment	N	S	W	E	C				
	0.001	Sat.	0.01	Sat.	0.00001	–	–	–	–

<sup>a</sup> The membrane used is Selemion CMV

<sup>b</sup> “Before” means before replacing the KCl solution in the W-compartment

<sup>c</sup> “After” means after replacing the KCl solution in the W-compartment

<sup>d</sup> Sat. means saturated KCl concentration

<sup>e</sup> P<sub>i-j</sub> represents the potential of i-compartment in reference to j-compartment

<sup>f</sup> The membrane used was Selemion CMV, same as the Experiment 1

<sup>g</sup> Concentration of KCl in individual compartments were the same as those employed in Experiment 2

<sup>h</sup> Time course of P<sub>N-S</sub> and P<sub>W-E</sub> are shown in Fig. 9

<sup>i</sup> Concentration of KCl in individual compartments were the same as those employed in Experiment 3

<sup>j</sup> Time course of P<sub>N-S</sub> and P<sub>W-E</sub> are shown in Fig. 10

<sup>k</sup> Individual compartments had KCl solutions concentrations of which were as shown in Experiment 5, which was the same as the KCl concentration before the disturbance induction in Experiment 4

<sup>l</sup> Time course of P<sub>N-S</sub> and P<sub>W-E</sub> are shown in Fig. 11

entire KCl solution in the W-compartment with new one due to the experimental difficulty, but most of the KCl solution in the W-compartment was replaced with new one. Experimental results of Experiment 1 in Table 1 suggest that only P<sub>W-E</sub> exhibited significant change after the disturbance, while the others were virtually not disturbed at all. Another experiment of Experiment 2 was carried out basically by the same procedure of Experiment 1. The exact experimental condition of Experiment 2 is summarized in Experiment 2 in Table 1. 0.01 M KCl solution was filled in the W-compartment before

the disturbance, while 0.001 M KCl solution was filled in the W-compartment in Experiment 1. Similar to the experiment 1, only P<sub>W-E</sub> exhibited significant change after the disturbance as shown in Experiment 2 in Table 1.

In Experiments 1 and 2, the potential of P<sub>N-S</sub> was generated through three compartments of N-, C-, and S-compartment, where this structure is hereafter called N-C-S system. The potential of P<sub>W-E</sub> was generated through three compartments, too, to be called W-C-E system in the same manner. Both systems had C-compartment in common. Since the

membranes of N-C and S-C are Selemon CMV, they are semi-permeable membranes. Therefore, the ion transport between N- and S-compartments as indicated by a fine solid arrow in Fig. 8 must have taken place for the generation of nonzero  $P_{N-S}$ . It suggests that GHK equation is applicable for explaining the potential generation of  $P_{N-S}$ . It is true for  $P_{W-E}$ , that is, the ion transport between W- and E-compartment must have taken place as indicated by a thick solid arrow in Fig. 8, and furthermore, it was expected that GHK equation could explain the potential generation of  $P_{W-E}$ . In this experimental system, ion fluxes indicated by fine and thick solid arrows must have existed. Thus, it was speculated that the ion fluxes of N-C-S system collided with those of W-C-E system in the C-compartment. Therefore, the disturbance of KCl solution condition in the W-compartment in both Experiments 1 and 2 had been the cause of the alteration of not only  $P_{W-E}$  but also  $P_{N-S}$ . However,  $P_{W-E}$  only was significantly altered after the induction of disturbance. Hence, it might be possible to derive a conclusion that the experimental observation in Experiments 1 and 2 were not explicable by an existing theory of GHK equation.

One might argue that the KCl condition of C-compartment has nothing to do with  $P_{N-S}$  and  $P_{W-E}$ , because of the following explanation based on existing theory of GHK equation. Equations (2) and (3) are derived by the use of GHK equation.

$$P_{N-C} = -\frac{RT}{F} \ln \left[ \frac{P_K [K^+]_N + P_{Cl} [Cl^-]_C}{P_K [K^+]_C + P_{Cl} [Cl^-]_N} \right] \quad (2)$$

$$P_{C-S} = -\frac{RT}{F} \ln \left[ \frac{P_K [K^+]_C + P_{Cl} [Cl^-]_S}{P_K [K^+]_S + P_{Cl} [Cl^-]_C} \right] \quad (3)$$

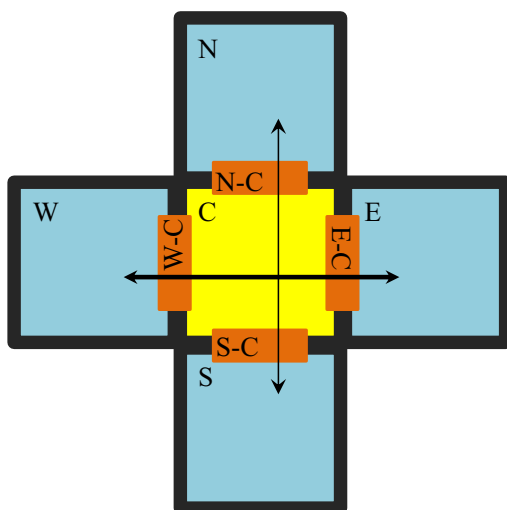


**Fig. 8** Ion transport passage. *Fine arrow* represents the ion transport passage for the generation of  $P_{N-S}$ . *Thick arrow* represents the ion transport passage for the generation of  $P_{W-E}$

$P_{N-S}$  is given by Eq. (4) using Eqs. (2) and (3).

$$P_{N-S} = P_{N-C} + P_{C-S} = -\frac{RT}{F} \ln \left[ \frac{P_K [K^+]_N + P_{Cl} [Cl^-]_C}{P_K [K^+]_C + P_{Cl} [Cl^-]_N} \right] - \frac{RT}{F} \ln \left[ \frac{P_K [K^+]_C + P_{Cl} [Cl^-]_S}{P_K [K^+]_S + P_{Cl} [Cl^-]_C} \right] \quad (4)$$

Selemon CMV is a cation exchange membrane. Thus, it is almost impermeable to anion,  $Cl^-$ . Since Selemon CMV was used as a membrane of N-C and S-C, the relation of  $P_K \gg P_{Cl}$  must be valid about Eq. (4). This kind of assumption was not uncommon in the electrophysiology field [17]. Hence, Eq. (4) is simplified as Eq. (5).

$$P_{N-S} \sim -\frac{RT}{F} \ln \left[ \frac{P_K [K^+]_N}{P_K [K^+]_S} \right] = -\frac{RT}{F} \ln \left[ \frac{[K^+]_N}{[K^+]_S} \right] \quad (5)$$

Equation (5) is interpreted as the concentration of C-compartment had nothing to do with  $P_{N-S}$ . With the same discussion, the concentration of C-compartment had nothing to do with  $P_{W-E}$ . Because of this explanation, it is possible to conclude at this moment that the membrane potential behavior summarized in Table 1 is explicable by GHK equation. Now, the author carried out the computation of potential  $P_{W-E}$  under the condition of Experiment 1 by employing the Eq. (6) derived by the same manner for deriving Eq. (5).

$$P_{W-E} \sim -\frac{RT}{F} \ln \left[ \frac{[K^+]_W}{[K^+]_E} \right] \quad (6)$$

It turned out that the  $P_{W-E}$ 's before and after the disturbance were  $\sim 210$  and  $\sim 0$  mV, respectively. Former computational potential was significantly different from the experimental value of 139 mV, but the latter computational potential was quite close to the experimental value of 4 mV. The same computational analysis was carried out under the experimental condition of Experiment 2. It turned out that the computationally obtained  $P_{W-E}$ 's before the disturbance and after the disturbance were  $\sim 150$  and  $\sim 0$  mV, respectively. Former computational potential was a bit different from the experimental value of 121 mV, and similarly, the latter computational potential was a bit different from the experimental value of 30 mV.

So, it was impossible to derive a firm conclusion about the membrane potential generation mechanism. Therefore, it was necessary to further proceed with some experiments to derive a firm conclusion. For the purpose of it, the experiment described in the “[Membrane potential in the middle of disturbance](#)” was carried out.

### Membrane potential in the middle of disturbance

The potential behavior described in the “**Membrane potential in equilibrium state**” was scrutinized further by carrying out another experiment under the same experimental condition as Experiment 2 in Table 1. But in this experiment,  $P_{N-S}$  and  $P_{W-E}$  were measured simultaneously as a function of time. Hereafter, this experiment is called Experiment 3, and its experimental condition is shown as Experiment 3 (same as Experiment 2) in Table 1. Figure 9 shows the experimentally obtained data curved of  $P_{N-S}$  and  $P_{W-E}$  vs. time, where the KCl solution in the W-compartment was replaced at the moment indicated by the arrow.

Right after the KCl solution replacement,  $P_{W-E}$  started lowering down and attained the stable potential in 11 s. During this 11 s, C-compartment was in transition state, and it was speculated that the solution condition such as ion fluxes of N-C-S system as well as W-C-E system were significantly altered. Therefore, it was expected that  $P_{N-S}$  would be disturbed to some extent at least in the period of the transition state, though the N-C-S system does not have the W-compartment. However, the data curve of  $P_{N-S}$  in Fig. 9 did not exhibit such a phenomenon but maintained a constant potential. This observation again cast a doubt on the validity of GHK equation. Still, one might argue that only a minute quantity of the saturated KCl solution filled in the W-compartment must have permeated through the membrane W-C into the C-compartment and such a minute quantity of saturated KCl concentration could not cause any influence on the condition of KCl solution in the C-compartment, since the concentration of C-compartment was as high as 1 M (see Experiment 3 in Table 1). Hence, still it is hard to derive some meaningful conclusion about the membrane potential generation mechanism. For compensating the shortcoming of Experiment 3, another experiment was carried out as described: The same experiment as Experiment 3 was carried out by intentionally employing quite low concentration 0.00001 M KCl solution for initially filling the C-compartment instead of 1 M KCl solution. Hereafter, this experiment is called Experiment 4,

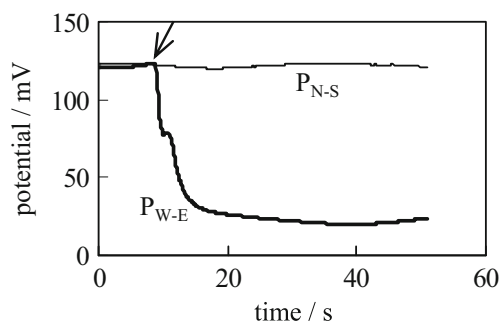


**Fig. 9** Time dependence of  $P_{N-S}$  (fine curve) and  $P_{W-E}$  (thick curve) under the experimental condition of Experiment 3 shown in Table 1. KCl solution replacement in the W-compartment was carried out at the moment indicated by the arrow

and its experimental condition is shown as Experiment 4 in Table 1. Even if the quantity of KCl solution permeating from the W-compartment into the C-compartment was quite small, KCl solution replacement in the W-compartment must have significant influence on the condition of the KCl solution in the C-compartment, since the initial concentration of KCl solution in the C-compartment was extremely low. Figure 10 shows the experimental result. Still, no variation of  $P_{N-S}$  was observed even at the transition state.

The experimental result of Experiment 4 again raises a doubt on the existing theory of GHK equation. But it needs to be careful for deriving a conclusion. If the experimental results of Experiments 3 and 4 could be interpreted as the quantity KCl solution permeating from the W-compartment into the C-compartment through the membrane of W-C was too small to induce the potential disturbance of  $P_{N-S}$  even in the transient state, those experimental results can be regarded as the phenomena within the range of existing theory of GHK equation. In order to clarify this point, the following experiment was carried out: The KCl concentrations of individual compartments in the experiment were initially the same as those of Experiment 4 before the replacement of KCl solution in the W-compartment. Hereafter, this experiment is referred to as Experiment 5, and the experimental condition is shown as Experiment 5 in Table 1. In Experiment 5, instead of replacing the KCl solution in the W-compartment, only a drop of saturated KCl solution was added into the C-compartment at the immediate neighbor of the membrane W-C. Then, the potentials  $P_{N-S}$  and  $P_{W-E}$  were measured as a function of time. Figure 11 shows the experimental result. Both  $P_{N-S}$  and  $P_{W-E}$  after the addition of only a drop of saturated KCl solution were significantly disturbed. The addition of a drop of KCl was done at  $t=0$  s. So, even the slight change of KCl concentration in the C-compartment could cause significant disturbance of  $P_{N-S}$  as well as  $P_{W-E}$ . Hence, a minute quantity of KCl solution migration into the C-compartment from the W-compartment might have caused a significant disturbance of potential in the experiments in Experiments 3 and 4, but actually, no potential

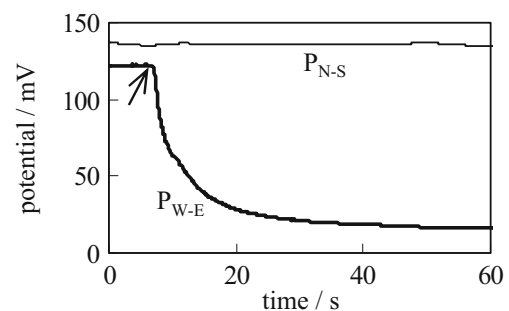


**Fig. 10** Time dependence of  $P_{N-S}$  (fine curve) and  $P_{W-E}$  (thick curve) under basically the same experimental condition as Fig. 9, but the KCl concentration in the C-compartment was 0.00001 M not 1 M KCl solution; replacement in the W-compartment was carried out at the moment indicated by the arrow

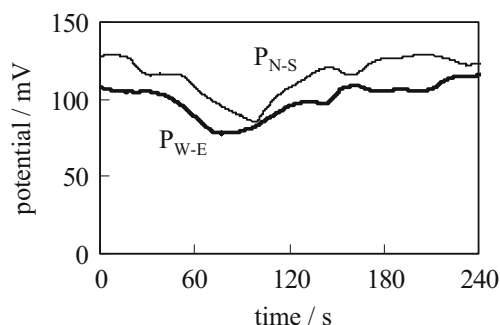


**Fig. 11** Time dependence of  $P_{N-S}$  (fine curve) and  $P_{W-E}$  (thick curve) after the addition of a drop of saturated KCl solution into the C-compartment at the immediate neighbor of the membrane W-C. The initial KCl concentration in the individual compartments and the membranes used were the same as those for Fig. 10

disturbance was observed about  $P_{N-S}$ . Therefore, it is strongly speculated that the membrane potential across the ion exchange membrane was caused not by ion transport through the membrane. This conclusion is in conflict with the prediction by GHK equation. The author does not say “Ion transport never took place in the experiments so far described”. What we would like to emphasize is “Ion transport must have taken place in any experiment described above, but the ion transport might not be the cause of potential generation. The potentials of  $P_{N-S}$  and  $P_{W-E}$  must have exhibited significant alteration by the disturbance, as long as the ion transport was the cause of potential generation”.

To sum up the experimental results introduced in the “Membrane potential across the semi-permeable membrane”, the potential generation mechanism between two compartments is not necessarily within the range of existing theory of GHK equation. Any theory as well as the GHK equation cannot account for the nonzero potential generation across the membrane, as long as the theory attributes the nonzero potential generation to the transmembrane ion transport. However, still, some may argue that all the above described experimental results are explicable by an existing theory of Donnan theory [1, 2, 4–6]. Since all the membranes, N-C, S-C, W-C, and E-C, were not as thin as actual cell membrane, even those membranes could be regarded as a phase with large enough thickness for ions such as  $K^+$ ,  $Cl^-$ , ... . Selemion CMV used as those membranes are not as thin as the actual cell membrane, and the thickness of Selemion CMV is around 120  $\mu m$  by far thicker than the actual cell membrane. In addition to that, Selemion CMV contains  $-SO_3H$  groups, which can dissociate into immobile fixed charge of  $-SO_3^-$  and mobile charge of  $H^+$ . Namely, Selemion CMV forms a phase containing fixed negative charge in it. Therefore, disparity of  $K^+$  and  $Cl^-$  concentration must have taken place among all the compartments and all the membranes according to the Donnan theory. It suggests that the generation of nonzero potential between any two compartments shown in Figs. 9, 10, and 11 is quite natural and nothing new from the standpoint of the Donnan

theory. However, in all the experiments so far described, there existed ion concentration gradient between any two compartments the author focused on. It suggests that there existed ion fluxes in the experimental systems. Applying Donnan theory to such a system with ion fluxes is inappropriate, but GHK equation should be used, as long as the existing theories are right. It is concluded that neither GHK equation nor Donnan theory can explain the experimental results so far shown.

Membrane potential across the impermeable membrane

*Potential across a liquid membrane containing either negatively or positively charged molecule*

Potential between two compartments separated by a liquid membrane was measured using the setup shown in Fig. 6. Im-N introduced in the “Membrane of N-C, S-C, W-C, and E-C” was prepared and was used as membranes of N-C, S-C, W-C, and E-C shown in Fig. 6. N-, S-, W-, and W-compartment were filled with the KCl solutions; the concentrations of which are shown in Experiment 6 in Table 2, where hereafter, this experiment is called Experiment 6. C-compartment was filled up with Im-N not KCl solution. Since all the membranes and the solution in the C-compartment were the same solution, they virtually formed a single membrane separating N-, S-, W-, and E-compartment to one another.  $P_{N-S}$  and  $P_{W-E}$  were measured as a function of time, and the result is shown in Fig. 12. Im-N is impermeable to water nor KCl. However, nonzero potentials,  $P_{N-S}$  and  $P_{W-E}$ , were generated and maintained constant. GHK equation is not applicable for explaining those nonzero potentials because of impermeability of Im-N to KCl.

Next, the Donnan theory could explain the nonzero potential generation. N-C-S system and W-C-E system had C-compartment in common, and KCl concentration in S-compartment is the same as that in E-compartment. Difference between those two systems lied only in the KCl concentration difference between N-compartment and W-compartment.

**Table 2** KCl concentration and the membrane used

Concentration of KCl (M)				
N	S	W	E	C
Experiment 6 <sup>a</sup>				
0.00001	Sat. <sup>b</sup>	1	Sat.	Im-N <sup>a</sup>
Experiment 7 <sup>c</sup>				
0.00001	Sat. <sup>b</sup>	1	Sat.	Im-P <sup>c</sup>

<sup>a</sup> The membrane used was Im-N. Im-N is a mixture of poly(ethylene glycol) 4-nonylphenyl 3-sulfopropyl ether potassium salt and 1-pentanol

<sup>b</sup> Sat. means saturate KCl concentration

<sup>c</sup> The membrane used was Im-P. Im-P is a mixture of 1-decyl-3-methylimidazolium chloride and 1-pentanol

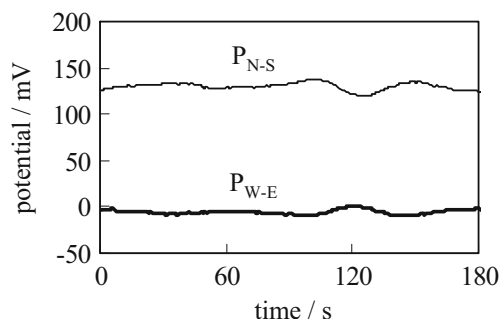


**Fig. 12** Time dependence of P<sub>N-S</sub> (fine curve) and P<sub>W-E</sub> (thick curve), where all the KCl solution was separated to one another with a liquid membrane lm-N

According to Fig. 12, the N-C-S system exhibited about 130 mV, while the W-C-E system exhibited about 0 mV. The potential difference between them was 130 mV–0 mV=130 mV and was caused undoubtedly by the KCl concentration difference between N-compartment and W-compartment. Potentials in the N- and C-compartments in reference to the S-compartment are denoted V<sub>N</sub> and V<sub>C</sub>, respectively, and those in the W- and C-compartments in reference to the E-compartment are denoted V<sub>W</sub> and V<sub>C'</sub>, respectively. Since the KCl concentration in S-compartment was the same as that in W-compartment, their electrochemical conditions were virtually the same in each other. Therefore, it is possible to derive the relationship of V<sub>C</sub>=V<sub>C'</sub>. Let's focus on the concentration of K<sup>+</sup> in each compartment. Though the C-compartment was filled with 1-pentanol impermeable to KCl, an extremely low quantity of K<sup>+</sup> could exist as a counter ion of PEG-K of lm-N. Based on the Donnan theory, [K<sup>+</sup>]<sub>N</sub>: [K<sup>+</sup>]<sub>C</sub> is given by Eq. (7), and [K<sup>+</sup>]<sub>W</sub>: [K<sup>+</sup>]<sub>C</sub> is given by Eq. (8), where e and k represent elementary charge and Boltzmann constant.

$$[K^+]_N : [K^+]_C = \exp\left[-\frac{eV_N}{kT}\right] : \exp\left[-\frac{eV_C}{kT}\right] \tag{7}$$

$$[K^+]_W : [K^+]_C = \exp\left[-\frac{eV_W}{kT}\right] : \exp\left[-\frac{eV_{C'}}{kT}\right] \\ = \exp\left[-\frac{eV_W}{kT}\right] : \exp\left[-\frac{eV_C}{kT}\right] \tag{8}$$

Equation (9) is derived by the use of Eqs. (7) and (8).

$$\frac{[K^+]_N}{[K^+]_W} = \exp\left[-\frac{e}{kT}(V_N - V_W)\right] \tag{9}$$

Similarly, Eq. (10) is obtained.

$$\frac{[Cl^-]_N}{[Cl^-]_W} = \exp\left[+\frac{e}{kT}(V_N - V_W)\right] \tag{10}$$

Since the liquid membrane is impermeable to water and KCl, it is quite plausible to believe that the concentration of K<sup>+</sup> and Cl<sup>-</sup> in the individual compartments were constant throughout the measurements. According to the experimental condition of Experiment 6, [K<sup>+</sup>]<sub>N</sub>/[K<sup>+</sup>]<sub>W</sub>=0.00001, [Cl<sup>-</sup>]<sub>N</sub>/[Cl<sup>-</sup>]<sub>W</sub>=0.00001, T=300 K, and V<sub>N</sub>-V<sub>W</sub>=130 mV. Right hand side of Eq. (9) is 0.0066 and that of Eq. (10) is 152 by computation, and they are totally different from the experimental conditions of [K<sup>+</sup>]<sub>N</sub>/[K<sup>+</sup>]<sub>W</sub>=0.00001 and [Cl<sup>-</sup>]<sub>N</sub>/[Cl<sup>-</sup>]<sub>W</sub>=0.00001, respectively. These results suggest that the Donnan theory is inappropriate as the explanation of potential generation cause. The computational results of [K<sup>+</sup>]<sub>N</sub>/[K<sup>+</sup>]<sub>W</sub>=0.0066 and [Cl<sup>-</sup>]<sub>N</sub>/[Cl<sup>-</sup>]<sub>W</sub>=152, which was derived based on the Donnan theory, is invalid in terms of macroscopic electroneutrality, too. It is detailed as follows: The liquid membrane is impermeable to water and KCl, [K<sup>+</sup>]<sub>W</sub> and [Cl<sup>-</sup>]<sub>W</sub> must have been constant, 1 M, throughout the experiment as described already. Thus, [K<sup>+</sup>]<sub>N</sub>=0.0066 M and [Cl<sup>-</sup>]<sub>N</sub>=152 M, as long as the Donnan theory is valid. The equation of electroneutrality in the N-compartment is given by Eq. (11).

$$e[K^+]_N + e[H^+]_N - e[Cl^-]_N - e[OH^-]_N = 0 \tag{11}$$

At the standard condition for temperature and pressure, proton concentration of water is around 10<sup>-6</sup>–10<sup>-5</sup> M. Hence, [H<sup>+</sup>]<sub>N}~10<sup>-6</sup>–10<sup>-5</sup> M. Since the ionization constant of water is 10<sup>-14</sup>, [OH<sup>-</sup>]<sub>N}~10<sup>-8</sup>–10<sup>-9</sup> M. [K<sup>+</sup>]<sub>N</sub>=0.0066 M as shown above, while [Cl<sup>-</sup>]<sub>N</sub>=152 M. So, plugging those quantities ([K<sup>+</sup>]<sub>N</sub>=0.0066 M, [Cl<sup>-</sup>]<sub>N</sub>=152 M, [H<sup>+</sup>]<sub>N}~10<sup>-6</sup>–10<sup>-5</sup> M, [OH<sup>-</sup>]<sub>N}~10<sup>-8</sup>–10<sup>-9</sup> M) into the left hand side of Eq. (11) cannot result in zero. The Donnan theory does not fulfill the requirement of macroscopic electroneutrality. Hence, the Donnan theory cannot be validated. This problem is well discussed by Dr. Ling as the violation of macroscopic electroneutrality of Donnan theory [1, 2, 5, 6].</sub></sub></sub></sub>

To sum up, neither GHK equation nor Donnan theory can explain the experimental result shown in Fig. 12. The same experiment was carried out by using a liquid membrane of lm-P, which was introduced in the “Membrane of N-C, S-C, W-C, and E-C”, in place of lm-N. The exact condition is given in experiment 7 in Table 2, where hereafter this experiment is called experiment 7. The experimental result is shown in Fig. 13. lm-P is impermeable to water and KCl as well. However, nonzero potentials, P<sub>N-S</sub> and P<sub>W-E</sub>, were generated and maintained constant. By the same argument for Fig. 12, neither GHK equation nor Donnan theory can explain the experimental result shown in Fig. 13. Therefore, a new concept is in need as a potential generation mechanism.

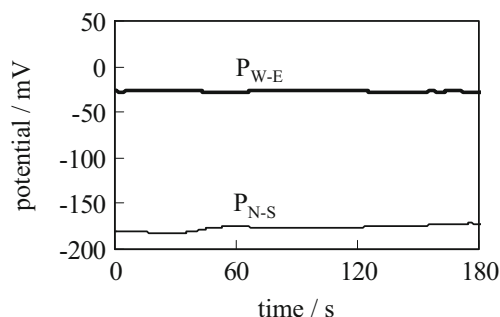


**Fig. 13** Time dependence of  $P_{N-S}$  (fine curve) and  $P_{W-E}$  (thick curve), where all the KCl solution was separated to one another with a liquid membrane lm-P

#### Potential across the liquid membrane bearing both negative and positive charges

Another potential measurement was carried out. In this experiment, all the compartments but C-compartment were filled up with KCl solutions and their concentration is summarized in Experiment 8 in Table 3. The membranes N-C and S-C were lm-P, while those of W-C and E-C were lm-N. All four membranes were connected with quite fine cotton thread as illustrated in Fig. 14. A small quantity of lm-P (of N-C and W-C) and a small quantity of lm-N (of W-C and E-C) were absorbed into the cotton thread autonomously. Therefore, all four membranes became electrically connected to one another through those fine threads. If thick threads had been used instead of fine threads, a large quantity of lm-N and lm-P would have been absorbed into the threads, and it could cause the heavy mixing of all four liquid membranes to one another, resulting in the contamination of membranes, N-C, S-C, W-C, and E-C. Therefore, fine threads were used.

Figure 15 shows the time dependence of  $P_{N-S}$  and  $P_{W-E}$ . Obviously, nonzero potentials were generated. Liquid membrane was primarily composed of 1-pentanol. Since both  $K^+$  and  $Cl^-$  were virtually insoluble to 1-pentanol, neither  $K^+$  nor  $Cl^-$  could be transported through the liquid membranes. Consequently, the generation of nonzero potentials of  $P_{N-S}$  or  $P_{W-E}$  is inexplicable by the GHK equation. The applicability of Donnan theory to this experimental result was considered next.

W-compartment was electrically connected with E-compartment using a fine thread, and this system is denoted W-T-E system from now, where T of W-T-E represents the fine thread containing lm-N and lm-P. W- and E-compartments and T-phase all contained  $K^+$ .<sup>1</sup> Potentials between W-compartment and T-phase and between T-phase and E-compartment are represented by  $P_{W-T}$  and  $P_{T-E}$ , respectively. According to the Donnan theory, the concentration ratio of  $K^+$

<sup>1</sup> Readers might think that T-phase did not contain  $K^+$  at all, since the author describes that 1-pentanol is impermeable to  $K^+$ . What the author emphasizes is that an extremely small quantity of  $K^+$  could exist into 1-pentanol, but virtually, it could be regarded that no  $K^+$  existed in 1-pentanol.

**Table 3** Concentration of KCl solution and liquid membranes used

Experiment 8								
Concentration of KCl (M)					Liquid membrane			
N	S	W	E	C	N-C	S-C	W-C	E-C
0.001	Sat.	0.001	Sat.	— <sup>a</sup>	lm-P	lm-P	lm-N	lm-N

<sup>a</sup> C-compartment was not filled with solution, but a cotton thread was placed in it

among individual compartments and phase is given by Eq. (12).

$$[K^+]_W : [K^+]_T : [K^+]_E = \exp\left[-\frac{e(P_{W-T} + P_{T-E})}{kT}\right] : \exp\left[-\frac{eP_{T-E}}{kT}\right] : 1 \quad (12)$$

Employing the experimental result of  $P_{W-T} + P_{T-E} = 100$  mV shown in Fig. 15,  $[K^+]_W/[K^+]_E = 0.02$  was obtained computationally. According to the data shown in Table 3, actual initial concentration ratio of  $K^+$  between W- and E-compartments was less than 0.0003, which is by far less than 0.02 computationally obtained. Of course, the initial concentrations of  $K^+$  in W- and E-compartments had been maintained throughout the potential measurement, since 1-pentanol is virtually impermeable to  $K^+$ . Therefore, the Donnan theory was ruled out as a cause of nonzero potential generation between W- and E-compartments. Since the GHK equation was ruled out, too, it was concluded that new concept was needed for the potential generation mechanism explanation.

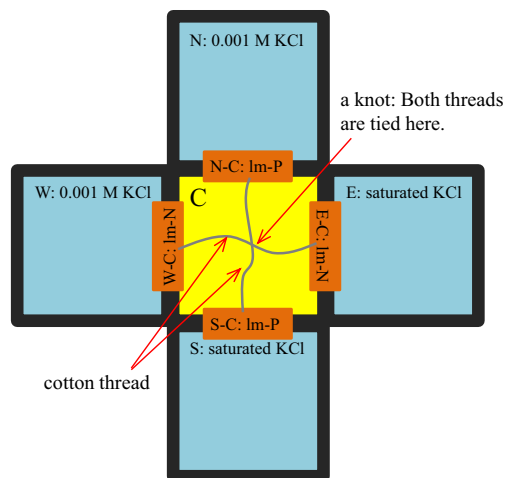


**Fig. 14** Experimental setup. All the compartments were separated by lm-N or lm-P as illustrated. All the membranes were connected with two fine cotton threads tied each other at the center of C-compartment

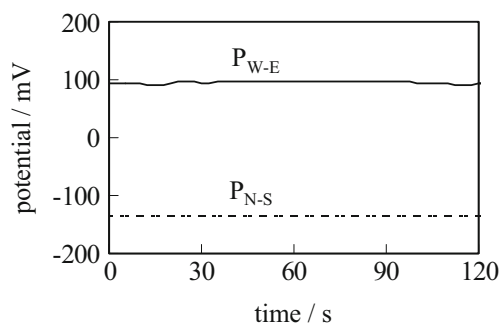


Fig. 15 Time dependence of  $P_{N-S}$  (dashed line) and  $P_{W-E}$  (solid line)

Alternative theory as the membrane potential generation mechanism

Potential across the liquid membrane

The experimental result of Fig. 15 was considered first. No existing theories appear to explain the results. Drs. Ling and Cheng have emphasized that the ion adsorption is the origin of membrane potential [1, 2, 5, 6, 9–13]. The interfacial molecular structure between the KCl solution and the liquid membrane can be illustrated as Fig. 16. Since DMIC in lm-P has a long hydrocarbon tail, a monolayer consisting of DMIC must have been formed at the interface between the KCl solution

and the liquid membrane. Its hydrocarbon chain was anchored in the membrane phase and the positively charged head of DMIC located in the KCl solution. So, the positively charged monolayer was formed at the interface between the KCl solution and liquid membrane as in Fig. 16.

$Cl^-$  in the KCl solution is adsorbed on the positively charged monolayer. According to the adsorption theory, the conditions (I) and (II) shown below must be established concerning the potential generation of  $P_{N-S}$  [1, 2, 5, 6, 9–13].

- (I) Anion,  $Cl^-$ , adsorption on the positively charged sites at the interface obeys the Langmuir isotherm.
- (II) Ion distribution in KCl solution phase obeys the Boltzmann distribution.

Then, the potential profile represented by the dotted curve shown in Fig. 17 was expected to form.  $\phi_N$  in Fig. 17 represents the potential in N-compartment at the position sufficiently away from the N-C in reference to the potential to the membrane phase.  $\phi_S$  in Fig. 17 represents the potential in S-compartment at the position sufficiently away from the S-C in reference to the potential to the membrane phase.  $P_{N-S}$  is given by the difference between  $\phi_N$  and  $\phi_S$  as shown in Fig. 17,  $P_{N-S} = \phi_N - \phi_S$ .

The author of this paper already derived a formula representing the potential by taking the Langmuir isotherm

Fig. 16 Interfacial molecular structure imagined between the KCl solution and the liquid membrane of lm-P

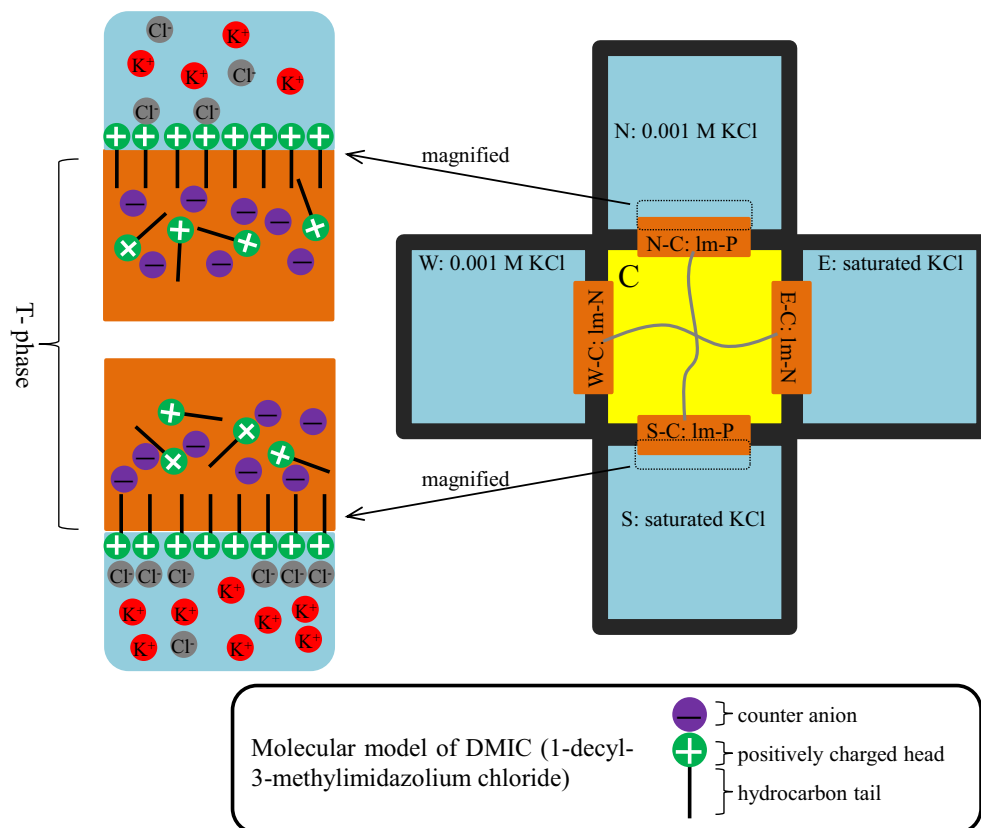
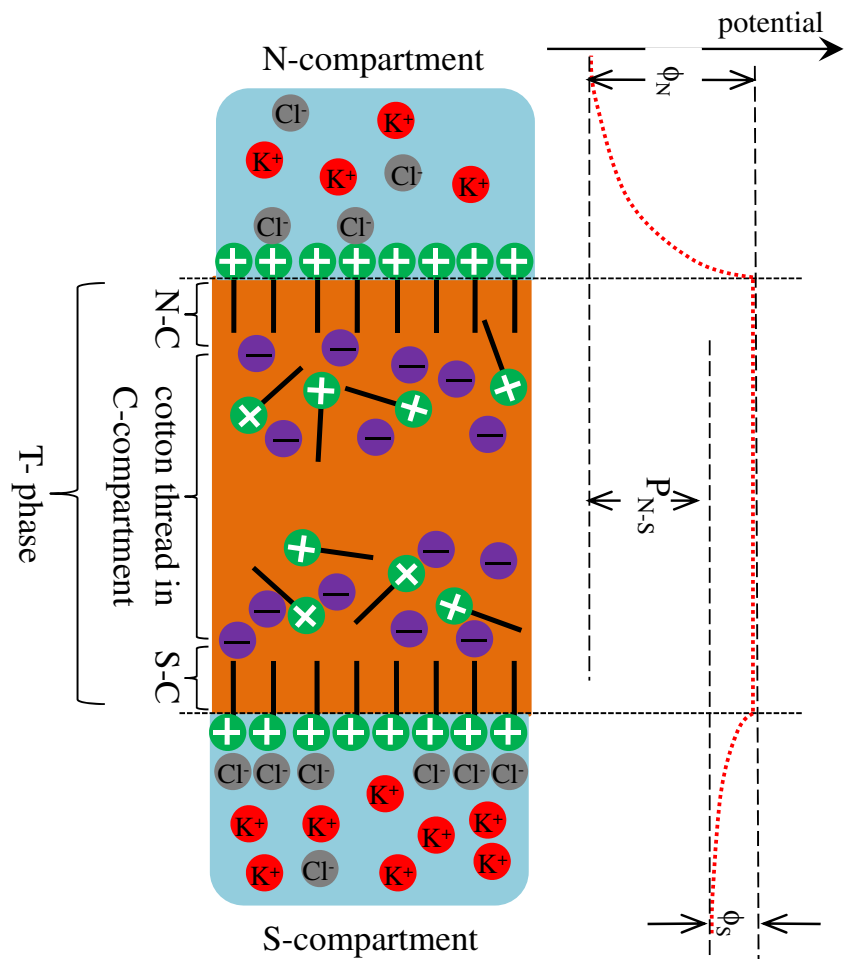


**Fig. 17** Potential profile from S-compartment to N-compartment



and the Boltzmann distribution into consideration under the constraint condition of electroneutrality [14]. Such an approach for deriving the formula of potential is the same as Drs. Ling's and Cheng's [1, 2, 5, 6, 9–13]. Applying the formula the author derived, for instance, to the system illustrated in Fig. 17 results in the potential expression given by  $\Delta\phi$ ,  $\Delta\phi = \phi_N - \phi_S$ , where  $\phi_N$  and  $\phi_S$  are respectively given below.

$$\phi_N = -\frac{2RT}{F} \ln \left[ -\frac{1}{2} \frac{K[s]_T}{1 + KC_N} \sqrt{\frac{eFC_N}{2\epsilon\epsilon_0RT}} + \sqrt{\left(-\frac{1}{2} \frac{K[s]_T}{1 + KC_N}\right)^2 \frac{eFC_N}{2\epsilon\epsilon_0RT} + 1} \right] - \frac{e}{\epsilon_{low}\epsilon_0} \frac{KC_N[s]_T d}{1 + KC_N} \quad (13)$$

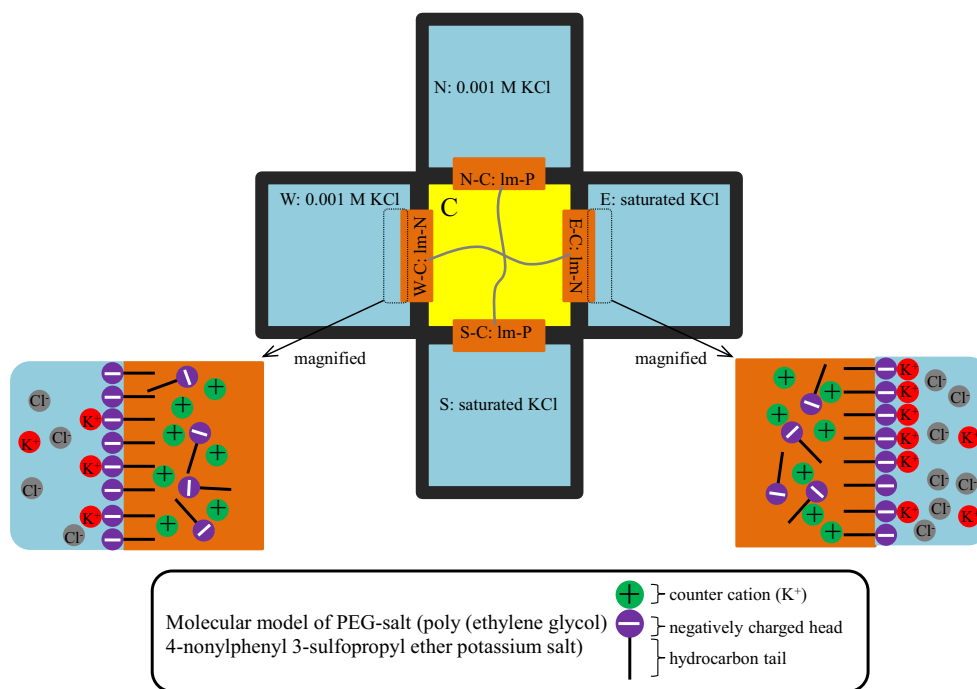
$$\phi_S = -\frac{2RT}{F} \ln \left[ -\frac{1}{2} \frac{K[s]_T}{1 + KC_S} \sqrt{\frac{eFC_S}{2\epsilon\epsilon_0RT}} + \sqrt{\left(-\frac{1}{2} \frac{K[s]_T}{1 + KC_S}\right)^2 \frac{eFC_S}{2\epsilon\epsilon_0RT} + 1} \right] - \frac{e}{\epsilon_{low}\epsilon_0} \frac{KC_S[s]_T d}{1 + KC_S} \quad (14)$$

R: gas constant, T: absolute temperature, F: Faraday constant,  $C_i$ : concentration of  $Cl^-$  at the bulk phase in the i-

compartment ( $i=N$  or  $S$ ),  $[s]_T$ : concentration of the adsorption site (positively charged monolayer) formed at the interface between T-phase and i-compartment ( $i=N$  or  $S$ ), K: association constant between the adsorption site and  $Cl^-$ , e: elementary charge,  $\epsilon_0$ : vacuum permittivity,  $\epsilon$ : relative permittivity of water,  $\epsilon_{low}$ : relative permittivity of water at the immediate neighbor of adsorption site, d: width of water phase with the relative permittivity  $\epsilon_{low}$ .

Based on the above equations, Eqs. (13) and (14), the potential in the KCl solution at the position sufficiently away from positively charged monolayer in reference to T-phase becomes lower as the KCl solution concentration decreases. As illustrated in Fig. 17, KCl concentration in N-compartment was lower than that in S-compartment. Therefore, it is expected that  $\phi_N$  is lower than  $\phi_S$ . Hence,  $P_{N-S}$  is negative as in Fig. 15 as expected. The same must be true for  $P_{N-S}$  and  $P_{W-E}$  in Experiment 7, since lm-P was used. In fact, both  $P_{N-S}$  and  $P_{W-E}$  were negative as in Fig. 13. The same discussion so far described is applicable to  $P_{W-E}$  in Fig. 15. The interfacial molecular structure imagined between the KCl solution and the liquid membrane is illustrated as Fig. 18. Since PEG-K in lm-N has long hydrocarbon tail, a monolayer consisting of

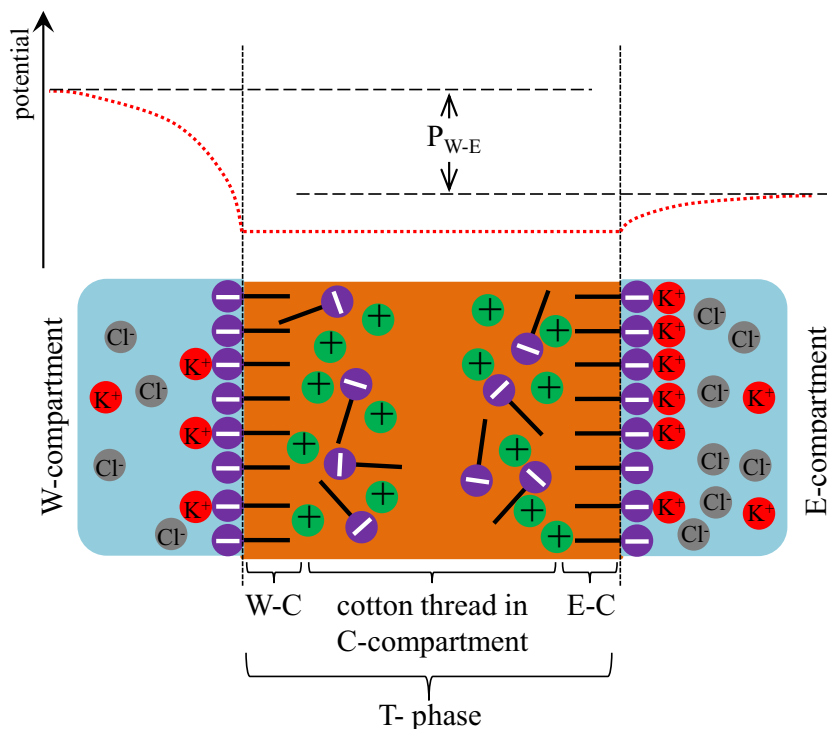
**Fig. 18** Interfacial molecular structure imagined between the KCl solution and the liquid membrane of Im-N



PEG-K must have been formed at the interface. Its hydrocarbon chain was anchored in the membrane phase, and its negatively charged head of the anchored PEG-K protruded in the KCl solution. So, the negatively charged monolayer was formed at the interface between the KCl solution and liquid membrane.  $K^+$  in the KCl solution was adsorbed on those negatively charged monolayer. The conditions (I) and

(II) must be fulfilled concerning the potential generation of  $P_{W-E}$  in Fig. 15. Then, the potential profile represented by the dotted curve showed Fig. 19 is expected to form. Based on the formula derived by the author [14], the potential in the KCl solution at the position sufficiently away from negatively charged monolayer in reference to T-phase becomes higher as the KCl solution concentration decreases.

**Fig. 19** Potential profile from E-compartment to W-compartment



Therefore,  $P_{W-E}$  in Fig. 19 is positive, and actual  $P_{W-E}$  shown in Fig. 15 was positive as expected. The same should be true for  $P_{N-S}$  and  $P_{W-E}$  in Fig. 12. In fact,  $P_{N-S}$  in Fig. 12 was positive, but  $P_{W-E}$  was not and slightly negative.  $P_{W-E}$  in Fig. 12 was generated, when KCl concentrations in W- and E-compartments were quite high of 1 M and saturated, respectively. Hence, there was not so large difference between those two KCl concentrations. Therefore,  $P_{W-E}$  slightly below zero was explicable by the adsorption theory as it was within the range of acceptable experimental error.

#### Reconsideration of potential across the ion exchange membrane

The potentials shown in Figs. 9 and 10, which were generated across ion exchange membranes, are reconsidered in this section employing the adsorption theory. The experimental result of Fig. 9 (Experiment 3) is reinvestigated under the adsorption theory. The ion exchange membrane used contains fixed  $-\text{SO}_3\text{H}$ . It dissociates into an immobile atomic group of  $-\text{SO}_3^-$  and a mobile cation of  $\text{H}^+$ . Based on the adsorption theory, the interfacial region between KCl solution and membrane is illustrated as Fig. 20.  $\text{K}^+$  is adsorbed to  $-\text{SO}_3^-$  of membrane of Selemion CMV at the interface between the KCl solution and membrane by obeying the Langmuir isotherm, and all the ions distribute according to the Boltzmann distribution [1, 2, 6, 9–14, 18–26].

Hence, prior to the induction of disturbance, the potential represented by the dotted line in Fig. 21a must have been generated between N- and S-compartments. The same argument is true for the potential generated between W- and E-compartments, and the dotted line in Fig. 21b represents the

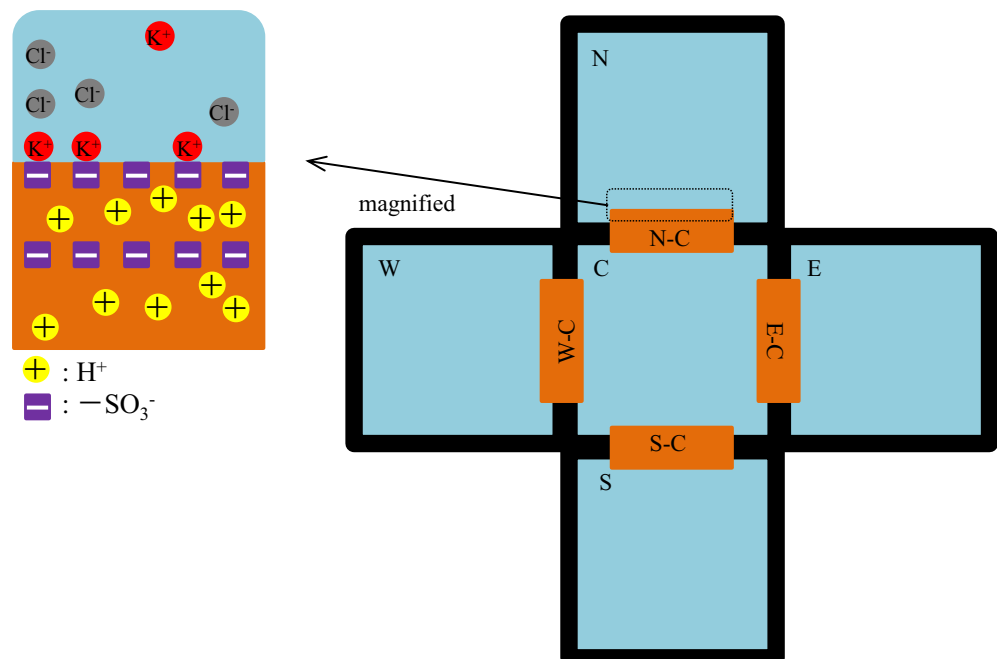
expected potential profile before the induction of disturbance. After the induction of disturbance, the condition (concentration of KCl and degree of ion adsorption) of individual compartments of N-C-S system was unaltered. However, the condition of W-compartment of W-C-E system was significantly altered, resulting in the diminish of potential in the W-compartment as illustrated in Fig. 21b, while the potential profiles in C- and E-compartments remain unaltered, where the solid curve in W-compartment represents the potential profile expected after the disturbance. Consequently,  $P_{W-E}$  diminishes after the induction of disturbance as illustrated in Fig. 21b. Eventually,  $P_{W-E}$  decreases as clearly seen in Fig. 21b. Therefore, the potential behavior shown in Fig. 9 was observed. Although the KCl concentration in the C-compartment in Fig. 10 (Experiment 4) was different from that in Fig. 9, basically, the same phenomenon as Fig. 9 must have occurred for Fig. 10.

To sum up, the adsorption theory appeared to be by far plausible than the existing theories for explaining the cause of membrane potential generation especially owing to the following points: (i) ion transport is not needed at all; (ii) electroneutrality is fulfilled; (iii) Boltzmann distribution, which is a quite basic concept of thermodynamics, is employed; and (iv) Langmuir isotherm, which is a quite basic concept of physical chemistry, is employed.

#### Validity of the foundation of this study

So far, we have emphasized that both GHK equation and Donnan theory have shortcomings for explaining the membrane potential generation behavior, and the author has advocated the adsorption theory as an alternative. It is known that

**Fig. 20** Interfacial structure imagined between N-compartment and N-C of Selemion CMV



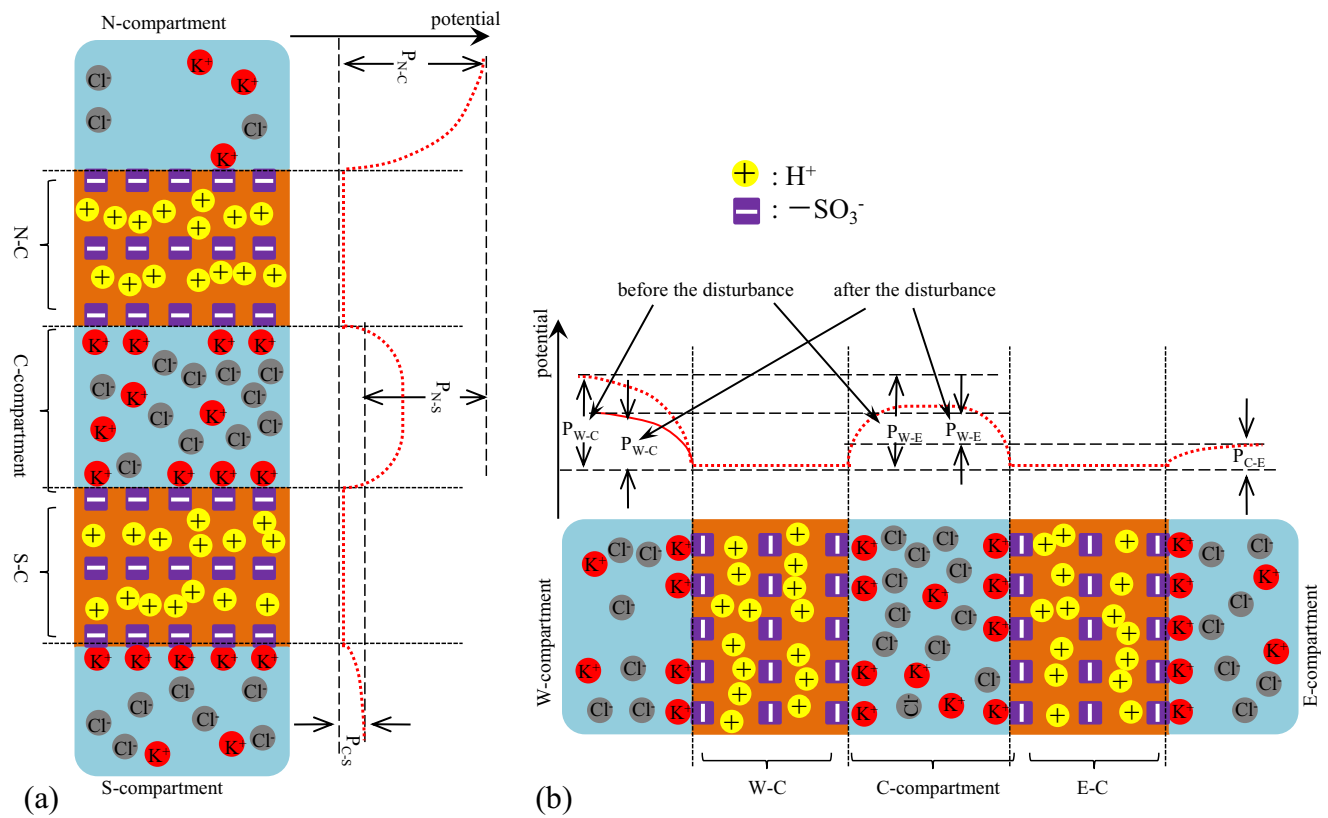


**Fig. 21** **a** Ion distribution and potential profiles in N-C-S for Figs. 9 and 10 before the induction of the disturbance. **b** Ion distribution and potential profiles in W-C-E systems for Figs. 9 and 10 before and after the induction of the disturbance

Donnan theory is applicable to the artificial system as well as living system (a cell) for explaining the potential generation behavior in those systems [1, 2, 4–6], although the use of Donnan theory was proved to be unsuitable for the artificial systems described in this study. Concerning the GHK equation, however, some readers of this paper might have a concern that the use of GHK equation for the analysis of potential behavior generated in the artificial system such as the setup employed in this study might be inappropriate, since the GHK equation is a strong mean for the prediction of real cell potential analysis in the physiology research field [1–3]. It is quite natural that such a concern is raised, since all the membranes employed in this work did not contain any functional molecule serving as an ion transporter at all, while it is usually explained that the cell potential is a consequence of transmembrane ion transport caused by the biological functional molecules embedded in the cell membrane such as an ion channel protein [1–3, 5–7]. Therefore, some readers might think that some part of the foundation of this work—to disprove the GHK equation by analyzing the potential behavior across the artificial membrane—is wrong in the first place. But the author of this paper would like to defy this kind of concern by the following discussion.

Contrary to our intuition, membrane potential-like phenomenon is observed not only in the living system of cell but also in the

nonliving artificial system. For example, Teorell reported the observation of action potential-like transmembrane potential in the artificially built system as early as 1959 [27]. He observed such a potential generated between 100 mM NaCl solution and 10 mM NaCl solution separated by a porous porcelain membrane after the imposed constant electric current across the membrane. Appropriately adjusting the magnitude of electric current imposed, even undamped action potential-like oscillatory potential was induced. Proteinoid-based microspheres are another artificially created system which exhibits membrane potential-like characteristics [28–31]. Proteinoid-based microspheres consist primarily of biological molecules of amino acids, but they are artificially created in a laboratory and do not contain any molecule playing a role of an ion transporter. However, the proteinoid-based microspheres bear characteristics of potential similar to the real cell membrane potential. Similar to the observation by Teorell described above, Ishima et al. observed action potential-like oscillatory potential in the proteinoid-based microsphere system [28]. What is quite intriguing is that such an action potential-like oscillatory potential was spontaneously induced without any external stimulation unlike Teorell’s observation. The study done by Yoshikawa et al. is even more intriguing [32, 33]. They made measurement of potential between 0.5 M NaCl solution and 0.5 M KCl solution separated by a porous membrane doped with Span-80. They experimentally observed that the action potential-like potential

oscillation spontaneously started without any external stimulation. On top of that, their experimental system used no biological materials unlike the proteinoid-based microsphere. Therefore, no functional molecules of ion transporter were employed in the study done by Yoshikawa et al.

It is not extreme to say that the membrane potential-like characteristics are not phenomena particular only to a real cell, but it is rather commonly observed phenomena even in artificially created systems. Therefore, the author believes that GHK equation should be applicable even to the artificial system, as long as it is applicable to a real cell system. As a matter of fact, there are no theoretical reasons that the GHK equation applicability is limited to the system consisting of biological living materials such as a living cell.

## Conclusion

Existing theories of the GHK equation nor the Donnan theory are not enough to fully explain the membrane potential behavior observed in the experiments shown in this paper. On the other hand, the adsorption theory is in harmony with those observations, and it is strongly backed by the quite fundamental scientific concepts in the thermodynamics and physical chemistry fields. It is strongly speculated that the adsorption theory provides with the real cause of membrane potential generation.

**Acknowledgments** This research was conducted under the financial support of the Ministry of Education, Science, Sports and Culture, Grant-in-Aid for Challenging Exploratory Research, 26650032, 2014.

## References

- Ling G (1991) Revolution in the physiology of the living cell. Krieger Pub Co, Florida
- Ling G (2001) Life at the cell and below-cell level: the hidden history of a fundamental revolution in biology. Pacific Press, New York
- Miyakawa H, Inoue M (2003) Nyuuron no Seibutsu-tsubuturi (Biophysics of neuron). Maruzen, Tokyo
- Hanai T (1978) Maku to Ion (Membrane and ions). Kagakudojin, Tokyo
- Mentré P (2006) Saibou no nakano mizu (Water in the cell) (Japanese translation of L'eau dans la cellule, Masson, Paris, 1996). University Tokyo Press, Tokyo
- Ling G (2011) Truth in basic biomedical science will set future mankind free. *Physiol Chem Phys Med NMR* 41:19–48
- Pollack GP (2001) Cells, gels and the engines of life. Ebner & Sons, Seattle
- Pollack GP (2013) The fourth phase of water: beyond solid, liquid, and vapor. Ebner & Sons, Seattle
- Cheng KL (1990) Capacitor theory for nonfaradaic potentiometry. *Microchem J* 42:5–24
- Huang C-M, Jean YC, Cheng KL (1995) Isotopic evidence disproving ion exchange reaction between  $H^+$  and  $Na^+$  in pH glass electrode. *J Electrochem Soc* 142:L175–L176
- Cheng KL (1998) Explanation of misleading Nernst slope by Boltzmann equation. *Microchem J* 59:457–461
- Temsamani KR, Cheng KL (2001) Studies of chloride adsorption on Ag/AgCl electrode. *Sensors Actuators B Chem* 76:551–555
- Cheng KL (2002) Recent development of non-faradaic potentiometry. *Microchem J* 72:269–276
- Tamagawa H, Morita S (2014) Membranes, membrane potential generated by ion adsorption. *Membranes* 4:257–274
- Colacicco G (1965) Electrical potential at an oil/water interface. *Nature* 207:936–938
- Colacicco G (1965) Reversal of potential across a liquid non-aqueous membrane with regard to membrane excitability. *Nature* 207:1045–1047
- Matsumoto G (1981) Phenomenon and substance of nerve excitation. (no English version but Japanese version only was published), Maruzen, Tokyo
- Plouraboue F, Chang H-C (2009) Symmetry breaking and electrostatic attraction between two identical surfaces. *Phys Rev E* 79: 041404
- Basuray S, Chang H-C (2010) Designing a sensitive and quantifiable nanocolloid assay with dielectrophoretic crossover frequencies. *Biomicrofluidics* 4:013205
- Anandarajah A, Chen J (1994) Double-layer repulsive force between two inclined platy particles according to the Gouy-Chapman theory. *J Colloid Interface Sci* 168:111–117
- Borukhov I, Andelman D, Orland H (2000) Adsorption of large ions from an electrolyte solution: a modified Poisson–Boltzmann equation. *Electrochim Acta* 46:221–229
- Chapot D, Bocquet L, Trizac E (2005) Electrostatic potential around charged finite rodlike macromolecules: nonlinear Poisson–Boltzmann theory. *J Colloid Interface Sci* 285:609–618
- Zhang J, Drechsler A, Grundke K, Kwok DY (2006) The similarity of electric double-layer interaction from the general Poisson–Boltzmann theory. *J Colloid Interface Sci* 300:391–395
- Polat M, Polat H (2010) Analytical solution of Poisson–Boltzmann equation for interacting plates of arbitrary potentials and same sign. *J Colloid Interface Sci* 341:178–185
- Alijó PHR, Tavaresa FW, Biscaia EC Jr (2012) Double layer interaction between charged parallel plates using a modified Poisson–Boltzmann equation to include size effects and ion specificity. *Colloids Surf A Physicochem Eng Asp* 412:29–35
- Trefalt G, Szilagyi I, Borkovec M (2013) Poisson–Boltzmann description of interaction forces and aggregation rates involving charged colloidal particles in asymmetric electrolytes. *J Colloid Interface Sci* 406:111–120
- Teorell T (1959) Electrokinetic membrane processes in relation to properties of excitable tissues I. experiments on oscillatory transport phenomena in artificial membranes. *J Gen Physiol* 42:831–845
- Ishima Y, Przybylski AT, Fox SW (1981) Electrical membrane phenomena in spherules from proteinoid and lecithin. *Bio Systems* 13: 243–251
- Przybylski AT, Stratten WP, Syren RM (1982) Fox SW membrane, action, and oscillatory potentials in simulated protocells. *Die Naturwissenschaften* 69:561–563
- Przybylski AT, Fox SW (1984) Excitable artificial cells of proteinoid. *Appl Biochem Biotechnol* 10:301–307
- Przybylski AT (1985) Excitable cell made of thermal proteinoids. *Biosystems* 17:281–288
- Yoshikawa K, Sakabe K, Matsubara Y, Ota T (1984) Oscillation of electrical potential in a porous membrane doped with glycerol  $\alpha$ -monoolate induced by an  $Na^+/K^+$  concentration gradient. *Biophys Chem* 20:107–109
- Yoshikawa K, Sakabe K, Matsubara Y, Ota T (1984) Self-excitation in a porous membrane doped with sorbitan monooleate (Span-80) induced by an  $Na^+/K^+$  concentration gradient. *Biophys Chem* 21:33–39